Contents lists available at ScienceDirect

Asian Pacific Journal of Tropical Medicine

journal homepage:www.elsevier.com/locate/apjtm

Document heading

Hsp90 inhibition induces destabilization of actin cytoskeleton in tumor cells: functional significance of Hsp90 interaction with F-actin

Vishal Chaturvedi, Amere Subbarao Sreedhar*

Centre for Cellular and Molecular Biology, Uppal Road, Hyderabad 500 007, India

ARTICLE INFO

Article history:
Received 2 July 2010
Received in revised form 28 July 2010
Accepted 15 August 2010
Available online 20 September 2010

Keywords:
Hsp90
F-actin
Cytoskeleton
17AAG
Tumor cells
Combination treatment

ABSTRACT

Objective: To examine the role of heat shock protein 90 (Hsp90) in the maintenance of actin cytoskeleton in human neuroblastoma tumor cells. **Methods:** Co-precipitation experiments were performed to examine Hsp90 interaction with actin. Hsp90 and actin interactions were evaluated by protein refolding and acto-myosin motility assays. 17-(Allylamino)-17-demethoxygeldanamycin (17AAG) induced actin-cytoskeleton re-organization was examined by laser scanning confocal microcopy. **Results:** It was shown that inhibition of Hsp90 by 17AAG accelerates detergent induced cell lysis of neuroblastoma tumor cells through destabilization of actin cytoskeleton. The *in vitro* co-precipitation experiments showed that functional but not mutant Hsp90 binds with F-actin. Among biochemical modifications, phopshorylation and oligomerization enhanced Hsp90 binding with F-actin. F-actin binding to Hsp90 interfered with Hsp90 chaperone activity in protein refolding assays, and Hsp90 binding to F-actin interfered with actin motility on myosin coated flow cell. In the combination treatment, 17AAG irreversibly augmented the effect of cytochalasin D, an inhibitor of actin polymerization. **Conclusions:** It can be concluded that Hsp90 binds to F-actin in tumor cells and maintains the cellular integrity. The results display a novel element of Hsp90 inhibition in destabilizing the actin cytoskeleton of tumor cells, therefore suggest that 17AAG combination with cytoskeletal disruptor may be effective in combating cancer.

1. Introduction

Cell movement through tissue plays a crucial role in cancer progression, and requires a series of distinct but concerted biological events in which the actin cytoskeleton play an essential role. The actin-mediated interactions not only perform mechanical functions supporting cell and tissue architecture but also transduce specific signals affecting fundamental biological functions[1,2]. Cytoskeleton is involved in all the aspects of cell behavior, which includes cancer and other human diseases[3,4]. The drugs that targets actin cytoskeleton serve as potential therapeutic agents in the treatment of cancer[5,6]. Current anticancer treatments aim to target tumor cells' ability to proliferate. Therapeutic drugs that target cell motility and invasion thus appear to be important to combat cancer. The microtubule affecting drugs are already considered to be promising tools to combat metastatic cancers[7,8].

Protein complexes play crucial role in several cellular functions, and heat shock proteins (Hsps) are central regulators of protein homeostasis. Very little information is available on Hsp dependency on actin and related folding complexes. Hsp60 homologue in the eukaryotes, TCP-1 is identified as a tubulin and actin binding protein[9,10]. Hsp70 was characterized as a microtubule-associated protein and is involved in tubulin polymerization. The Hsc70 cognate form found co-precipitated with both polymerized and depolymerized tubulin[11]. Small heat shock proteins help in recovery of actin[12]. The Hsp90 chaperone also thought to be involved in both microtubule-based functions and intermediate filaments[13,14]. Among different Hsps, Hsp90 chaperone is an abundant, ubiquitously expressed and highly conserved protein that is involved in a diverse array of cellular processes[15,16]. In mammalian cells, Hsp90 is associated with proto-oncogene kinases thus helps in tumor progression and cell survival. For this reason Hsp90 emerged as an exciting new target for the development of innovative cancer therapeutics[17,18]. Most of the antitumor

*Corresponding author: A. S. Sreedhar, Centre for Cellular and Molecular Biology Uppal Road, Hyderabad 500 007, India.
Tel: +91-040-27192698
Fax: +91-040-27160591
E-mail: assr@ccmb.res.in

effects of Hsp90 inhibition using geldanamycin and its analogue 17-(Allylamino)-17-demethoxygeldanamycin (17AAG) were attributed either to induce cytostasis or apoptosis. Therefore, a possible interaction between Hsp90 and actin polymers can be anticipated.

Remodeling of cytoskeleton usually results in loss of cell-cell communication and migration[19,20]. Further it was shown that disruption of microfilaments/intermediate filaments but not disruption of microtubules affects the metastatic ability of tumor cells. Heat shock proteins binding to cytoskeletal proteins has been shown to assist in trafficking of cellular proteins[21,22]. Although Hsp90 is localized to microtubules and microfilaments in live cells, though actin interferes with Hsp90 adenosine tri-phosphate (ATP) binding *in vitro*, a direct association between cellular actin with Hsp90 is not known. The aim of the present study was to examine the effect of Hsp90 inhibition on actin-cytoskeleton of tumor cells and to understand the significance of Hsp90 interactions with filamentous actin. We demonstrate that Hsp90 is indispensible for maintenance of actin-cytoskeleton in tumor cells.

2. Materials and methods

2.1. Materials

17AAG was purchased from Invivogen and Sigma respectively. Stock solutions of 17AAG (2 mg/mL) in DMSO and curcumin (10 mg/mL) in methanol were prepared. Dulbecco's Modified Eagles Medium (DMEM), fetal calf serum (FCS), penicillin, streptomycin, trypsin were purchased from GIBCO BRL. 4′,6-diamidino-2-phenylindole (DAPI), rhodamine phalloidin, Oregon green phalloidin were from Invitrogen-Molecular Probes. All other chemicals were from Sigma Chemical Company unless otherwise indicated.

2.2. Cell culture maintenance and treatments

Human neuroblastoma tumor cells (IMR32), rat fibroblasts (F111) and human cervical cancer cells (HeLa) were maintained in DMEM containing 10% FCS, penicillin (100 U/mL), and streptomycin (50 μg/mL) in a humidified atmosphere of 95% air and 5% CO_2 at 37 ℃. The exponentially growing tumor cells (1×10^6/mL) in the complete medium were used for drug treatments.

2.3. The morphological analysis and laser scanning confocal microscopy

Cells grown on cover glass (Fisher Scientifics, 22 mm× 22 mm) and treated with different drugs for different time intervals were visualized under phase contrast microscope (Nikon, TMS) attached to a 35 mm camera and photographed at 10× magnification for morphological analysis. For confocal microscopic analysis, cells were washed and fixed with 4% formaldehyde (10 min; room temperature) and permeabilized with 0.01% Triton X-100 (5 min). The actin cytoskeleton was stained using either rhodmaine labelled phalloidin or Oregon green labelled phalloidin (15 min; room temperature) and mounted onto the glass slide(s) along with ProLong Antifade reagent containing DAPI (50 nM; Invitrogen). The edges of the cover glasses were sealed to the slide with nail paint and observed under laser scanning confocal microscopy (Olympus FV500 microscope).

2.4. Lactate dehydrogenase measurement

The activity of lactate dehydogenase (LDH) was measured using the direct spectrophotometric assay in the presence of pyruvate and NADH. Tumor cells were treated with different concentrations of 17AAG for 6 h and subjected to 0.001% Brij58 treatment for another 10 min, centrifuged at low speed (3000 rpm; 5 min) using Remi table top centrifuge. The supernatant was collected and used for measuring the per cent LDH release from the cytosol. Complete cell lysis was achieved sonicating cells for 3 min, in three intervals, on ice. In 2 mL of 50 mM Hepes buffer (pH 7.4) containing 30 μM pyruvate and 30 μM NADH, 10 μL of supernatant was added, and changes in optical density was measured at 340 nm for 5 min. The percent LDH release was calculated by dividing the activity of LDH in the supernatant by the LDH activity measured after complete lysis achieved by sonication.

2.5. Purification of Hsp90 from rat liver

The 90 kDa heat shock protein was purified from rat liver with consecutive chromatographies on Butyl-Sepharose 4B, DEAE-Sepharose Fast Flow, Sephacryl S-200 and Econo-Pac HTP. The purity of these Hsp90 preparations was more than 95% as judged by silver staining of SDS polyacrylamide gels. Protein concentrations were determined according to Bradford method. N-terminal ATP-binding region deleted, bacterially expressed recombinant chicken Hsp90 protein was a kind gift from Dr. Yoshihiko Miyata, Japan.

2.6. Purification of Hsp90 from tumor cells

Hsp90 was purified from tumor cells in a single step ATP-sepharose chromatography. Two milliliter syringe was packed with pre-swollen ATP-sepharose, blocked with bovine serum albumin (1 mg/mL) to prevent non-specific binding to the sepharose matrix. Columns were pre-treated with ATP and NaCl (10 mM and 0.5 M respectively) and re-equilibrated with several bead volumes of binding buffer provided by the manufacturer. The crude cell lysates of control and 17AAG treated neuroblastoma cell extracts were passed over the column, and eluted with 10 mM ATP and 0.5 M NaCl. Hsp specific enhanced protein binding was achieved by omitting ADP from the binding buffer. Hsps including the major fraction of Hsp90 were eluted out with 10 mM ADP buffer, checked for its chaperone activity and used for F-actin binding assay.

2.7. Purification of actin from rabbit skeletal muscle

Actin was purified from rabbit skeletal muscle. Purified actin was always stored on ice at 4 ℃. The monomeric actin was polymerized for 1 h at room temperature in 5 mM Tris-

Cl, 50 mM KCl, 5 mM β-mercaptoethanol, 2 mM $MgCl_2$, and 1 mM ATP. The filamentous actin (F-actin) stock solution (23 μM) was stored at 4 ℃. The state of the actin was evaluated by SDS-PAGE and coomassie blue staining.

2.8. Hsp90-actin binding assay (co-precipitation and sedimentation)

Hsp90 and F-actin were used in 5 μg and 25 μg (1:5 ratio) respectively in 50 μL binding buffer containing 200 μM KCl, 5 μM $MgCl_2$, 2 μM DTT, and 40 μM Hepes (pH 6.8). The reaction mixture was incubated for 45 min at room temperature and centrifuged (Beckmen Centriguge, 100.1 rotor) at 53000 rpm for 1 h at 4 ℃. Supernatant and pellet fractions were separated, 6 μL supernatant was directly mixed with Laemmli buffer, whereas pellet is first suspended in 1% SDS and mixed with Laemmli buffer before loading onto 10% SDS-PAGE. Gel was allowed to run for one and half hour at constant voltage (160 V), after the run, the gel stained with coomassie blue and destained with acetic acid: methanol (10:50), and photographed.

2.9. In vitro phopshorylation and oligomerization of Hsp90

Phosphorylation of purified Hsp90 was carried out by incubating 5 μg of protein in 35 μL of kinase buffer (20 mM Tris-HCl, pH 7.2, 20 mM KCl, 10 mM $MgCl_2$, 60 mM NaCl, 10 mM sodium metabisulfate, 20 mM β-glycerophosphate, 6 mM EDTA, 6 mM p-nitro-phenyl-phosphate, and 1 mM dithiothreitol) containing 7 μCi of[γ-32P] ATP and 1 unit of casein kinase II for 15 min at 37 ℃. The dephosphorylation was achieved by treating Hsp90 with calf intestine alkaline phosphatase under respective buffering conditions provided by the manufacturer (Promega). Phosphorylation and dephosphorylations were confirmed by presence or absence of radioactivity (assayed by liquid scintillation counting). Hsp90 oligomerization was induced by subjecting the native Hsp90 protein purified from rat liver to heat stress at 42 ℃ for 20 min, oligomers were resolved on 4% native acrylamide gel, oligomerization was confirmed and the oligomerized Hsp90 protein used for subsequent experiments.

2.10. Luciferase renaturation assay

Luciferase was dissolved in stability buffer supplied by the manufacturer (Sigma) at a concentration of 0.5 mg/mL and denatured by heat shock at 41 ℃ for 10 min. Diluted rabbit reticulocyte lysate (10 μL) was dispensed to a 96-well plate (NUNC) and the refolding reaction was initiated by injecting 10 μL of the denatured luciferase mix to each well to give the following final concentrations: 20 mM Tris pH 7.7, 3 mM ATP, 5 mM creatine phosphate, 2.0 mM Mg(OAc)2, 75 mM KCl, 0.2 mg/mL CPK (creatine phospho kinase) and 1.5 μg/mL denatured luciferase. Plates were centrifuged for one min to assure complete mixing of the components. After incubation at room temperature for 3 h, luciferase activity was measured by injection of 40 μL of assay buffer (75 mM Tricine-HCl (pH 7.8), 24 mM $MgSO_4$, 0.3 mM EDTA, 2 mM DTT, 313 μM D-luciferin, 640 μM coenzyme A, 0.66 mM ATP, 150 mM KCl, 10% (v/v) Triton X-100, 20% (v/v) glycerol and 3.5% DMSO). Light emission from each well was read with a 10 sec integration time using a Perkin-Elmer EnVision 2101 plate reader. To study actin interference, 2 μg of F-actin or globular actin (G-actin) or both were used. ATP or apyrase enzyme was used as controls in place of 17AAG.

2.11. Citrate synthase renaturation assay

Chaperone activity was determined by the citrate synthase (CS) assay and the procedure was similar to luciferase assay except that CS aggregation was measured with light scattering at 360 nm for 30 min using spectrophotometer (Perkin Elmer). First 2 mg/mL CS was denatured by 8 M urea and 40 mM DTT treatment for 20 min, and the light scattering obtained was recorded. The denatured CS was diluted (1:50) with Tris.Cl buffer, pH 7.6 and the Hsp90 chaperone activity assays were performed at least thrice with preparations from independent purifications. Oxidized glucose-6-phosphate dehydrogenase (GAPDH) was used to compare the Hsp90 selective chaperoning functions with actin and citrate synthase. Commercially available GAPDH (2 mg/mL; Sigma) in 10 mM Hepes buffer (pH 7.6) was subjected to oxidation with 5 mM $FeSO_4$ and used.

2.12. In vitro actin motility assay and epifluorescence microscope

Actin filament movement on myosin-coated surface was studied in the presence and absence of Hsp90. The flow-through chamber was made sandwiched with two coverslips coated with heavy meromyosin (HMM; Sigma). The flow cell was first equilibrated with an HMM buffer (100 μg/mL, 25 mM KCl, 25 mM Imidazole, 1 mM EGTA, 4 mM $MgCl_2$, 1 mM DTT, pH 7.4). Then, the same buffer, to which 0.5 mg/mL bovine serum albumin was added, was perfused through the cell to remove unbound HMM and to block any exposed nitrocellulose. Actin filaments (60 ng/mL) were labeled with tetramethyl rhodamine-phalloidin (Molecular Probes, Eugene) in assay buffer (25 mM KCl, 25 mM Imidazole, 1 mM EGTA, 4 mM $MgCl_2$, 1 mM DTT, pH 7.4) was introduced into the flow cell. The buffer contained an oxygen scavenger system (0.1 mg/mL glucose oxidase, 0.018 mg/ml catalase, 2.3 mg/mL glucose) to retard photobleaching. Finally, 100 μL of assay buffer containing 1.0 mM ATP was flushed through the flow cell to initiate actin-filament motion. Actin filament velocities were determined by computer assisted program attached to the laser scanning confocal microscope. All experiments were performed at 30 ℃. Five micro moles of purified Hsp90 or 17AAG was added to the flow cell to study the actin motility inhibition.

2.13. Statistical analysis

Data presented as means±SD of minimum of three independent experiments unless otherwise indicated, and analyzed with Student's t test and a P value <0.05 was accepted significance. P values represented are, * for P< 0.05, ** for P< 0.01, *** for P<0.001.

3. Results

3.1. Hsp90 inhibition accelerates detergent induced cell lysis and induces cytoskeletal destabilization

Partial cell lysis was adapted to assess the cellular integrity. The neuroblastoma cells after 17AAG treatment were subjected to mild detergent lysis, and the percent LDH release was measured. The detergent concentration was standardized in such a way that it induces a minimum of 10% cell lysis in untreated cells. We observed a gradual increase in released LDH levels after 17AAG treatment which was concentration dependent. A 2 μM 17AAG treatment showed 38% cell lysis (Figure 1A; $P< 0.001$) that was increased to 65% in a 10 μM concentration. These results suggested 17AAG affects the cellular integrity. Since cellular integrity is associated with intact cytoskeleton, we first examined for cell morphology after the drug treatment, and observed altered cell morphology. Further to examine whether cell morphological alterations are due to gross re-arrangements of actin filaments, cells were stained with rhodmaine phalloidin and observed under a fluorescence microscope. A conspicuous destabilization of actin-cytoskeleton was observed after 17AAG treatment with change of a definite actin bundling at the plasma membrane to distorted F-actin arrays moving away from the plasma membrane (Figure 1B).

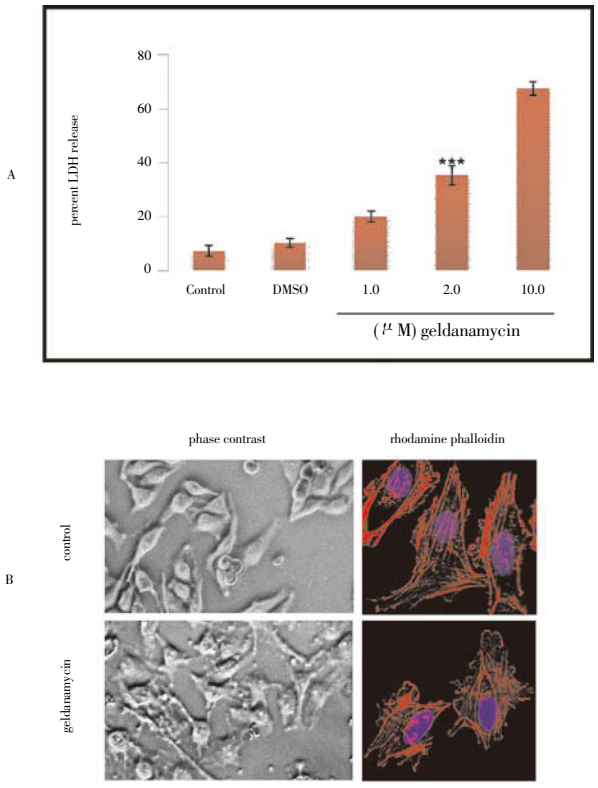

Figure 1. Geldanamycin induced effects on cellular integrity and actin-cytoskeleton.
A: Geldanamycin induced enhancement of detergent induced cell lysis. B: Geldanamycin induced cell morphology and destabilization of actin cytoskeleton.

3.2. The in vitro binding assay of purified Hsp90 and filamentous actin

We adapted *in vitro* spin-down assay to examine actin interaction with Hsp90. The purpose of this assay is to obtain a quantitative value of actin polymer for Hsp90 binding. Hsp90 and actin proteins were purified as explained in materials and methods. From *in vitro* sedimentation assay, we observed only functional Hsp90 binding to F-actin, however mutated Hsp90 did not show F-actin binding. Besides, functional Hsp90 has also co-precipitated with G-actin, however with a threefold difference with F-actin. More interestingly, though mutant Hsp90 failed to show any interaction with F-actin, it showed interaction with G-actin (Figure 2A).

3.3. Effect of Hsp90 biochemical modification on actin co-precipitation

To examine whether functional Hsp90 is obligatory for F-actin binding, we studied the effect of 17AAG (36 μM) and ATP (5 mM) on actin binding. The drug and ATP concentrations were standardized such that they inhibit *in vitro* chaperone activity of Hsp90 by at least 90% in a glucose-6-phosphate dehydrogenase (GAPDH) renaturation assay with re-constituted Hsp90 chaperone system (data not shown). These drugs were included in the assay mixture to inhibit Hsp90 and examined for Hsp90 binding to actin. Neither 17AAG nor ATP was found to interfere with F-actin binding to Hsp90 (Figure 2B) suggesting Hsp90 binding to F-actin could be independent of its chaperone activity. Hsp90 is a phosphoprotein and its phosphorylation is linked to chaperone activity, hence in the present study, Hsp90 was *in vitro* phosphorylated by casein kinase system as explained in materials and methods and phosphorylated Hsp90 was examined for actin binding. An increased binding of phosphoryled Hsp90 to F-actin was observed and in contrary, the dephopshorylation showed no effect on actin binding. The phosphorylation also failed to persuade G-actin binding with Hsp90 (Figure 2C).

Hsp90 is a dimeric protein with two independent substrate and ATP binding sites and its oligomerization was shown to enhance Hsp90 activity, therefore we examined Hsp90 oligomerization on F-actin binding. Hsp90 oligomerization was induced by heat stress as explained in materials and methods and oligomerization was confirmed by resolving the protein on a native gel (Figure 2D). The dimers and oligomers of Hsp90 were examined for F-actin binding. Compared to Hsp90 dimers, Hsp90 oligomers showed enhanced F-actin binding (Figure 2E) with a 0.5 fold ($P<0.001$) increase in Hsp90 protein and 1.6 fold ($P<0.001$) increase in F-actin (Figure 2F).

3.4. Actin interferes with Hsp90 chaperone function

In a pure system, it is difficult to evaluate functional significance of protein-protein interaction. Therefore we extended our study to understand the functional significance of Hsp90 interaction with F-actin using rabbit reticulocyte lysate (RRL) as chaperone system in the refolding assay of thermally unfolded luciferase. In control system the recovery obtained was maximum 93% in a 4 h time interval, whereas depletion of ATP using apyrase enzyme has completely inhibited its recovery. The reaction mixture supplemented

with G-actin inhibited luciferase refolding by a large extent (67%) whereas filamentous actin (F-actin) inhibited this by 53% (P<0.05), and the combination of F- and G-actin accelerated the inhibition of luciferase refolding by 82% (Figure 3A). Since luciferase refolding assay was an end-point measurement, which will not provide information on kinetic behavior of Hsp90 and actin interaction, we adapted citrate synthase refolding assay. We observed that F-actin more specifically interferes with citrate synthase renaturation compared to G-actin. Between G- and F-actin, 14% increased interference was observed with F-actin (Figure 3B).

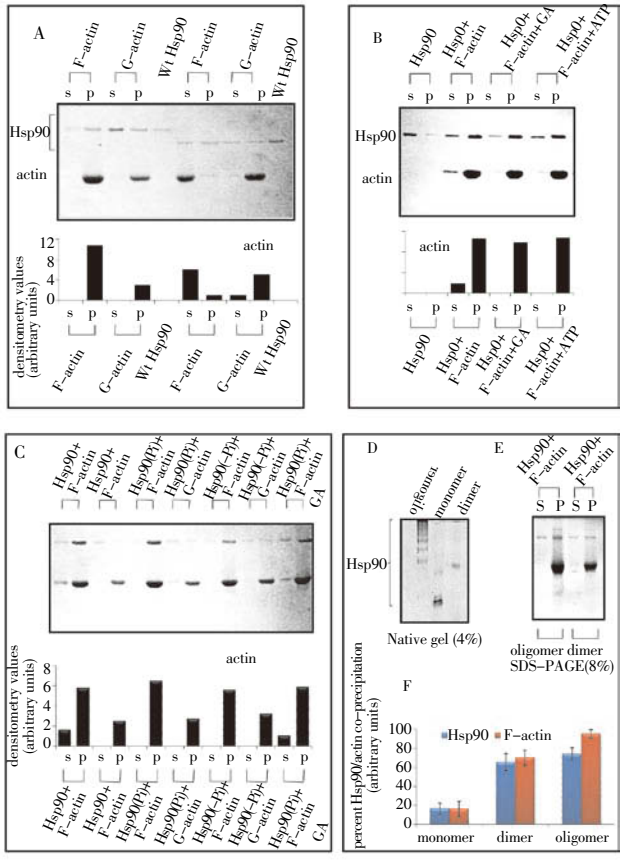

Figure 2. Hsp90 and actin *in vitro* binding assays.
P-pellet fraction; S-supernatant fraction. A: The *in vitro* co-precipitation assay to examine actin binding to functional (wt Hsp90) and mutant Hsp90 (mt Hsp90). B: nhibition of Hsp90 chaperone function on F-actin binding. C: Hsp90 phosphorylation effect on actin binding. D, E, and F: Effect of Hsp90 oligomerization on actin binding.

3.5. Hsp90 impedes actin motility on myosin coated plates

The renaturation experiments provided information on actin interference with Hsp90 chaperone activity but not on actin function. In a cellular system actin along with motor protein, myosin contracts, thus, mimics the simplified model of muscle force and motion generation. In the present study, we examined the effect of Hsp90 on actomyosin motor assay. In this assay, actin filament velocities were determined by computer assisted software and plotted as percent actin filament motility. Actin velocities were compared with functional Hsp90, mutated Hsp90 (△ATP), ATP and 17AAG supplements. We observed that Hsp90 addition to the reaction mixture decreased actin velocity by 52% (P< 0.01), and the mixture of Hsp90 and 17AAG reduced this inhibition to 28% (P<0.05). The mutated Hsp90 was found to be ineffective to impede actin motility on myosin coated plate (Figure 4A).

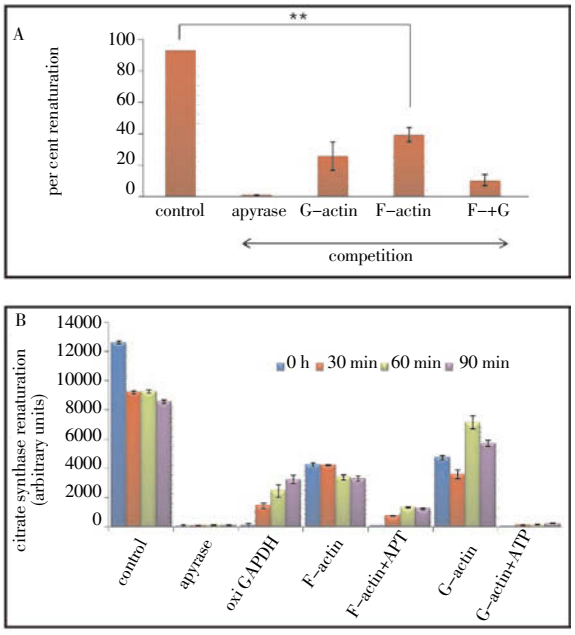

Figure 3. Analysis of actin binding and interference in Hsp90 functional assay.
A: Actin interference in the Hsp90 induced luciferase refolding. B: Kinetic analysis of Hsp90 mediated citrate synthase renaturation and actin interference.

3.6. The F-actin binding assay with normal and tumor Hsp90

From the studies above, one would argue that *in vitro* conditions tested with purified Hsp90 may not be the same with *in vivo* status. Therefore, we purified Hsp90 from using ATP-sepharose column from human neuroblastoma cells, and examined for F-actin binding. More than two fold increase of F-actin binding to Hsp90 was observed compared to normal cells (Figure 4B).

3.7. 17AAG induces time-dependent effect on actin-cytoskeleton: a kinetic analysis

Oregon green is more photo-stable and exhibit less pH sensitivity compared to rhodmaine-phalloidin which was used in our earlier experiments (Figure 1B), therefore in the present experiment rhodmaine phalloidin was replaced with oregon green phalloidin. Decreased F-actin arrays and actin bundling was observed by 6 h 17AAG treatment. More significantly we observed disappearance of stiffened F-actin filaments into irregular and curved filaments with reduced actin bundling. By 12 h 17AAG treatment cells lost their original architecture which exhibited constricted actin-cytoskeleton with massively re-organized F-actin arrays, and at this time interval, F-actin bundles

are majorly restricted to the plasma membrane. A 24 h treatment showed re-appearance of actin bundling and F-actin arrays, however, actin recruitment and periphery distribution was completely lost in tumor cells at this time interval. Additionally, we found lamellipodia formation with branched actin filaments in place of actin bundling (Figure 5). We evaluated 17AAG effect on other transformed cell types such as human cervical cancer cells, human glial cells and human T-lymphocytes (data not presented), and obtained similar results suggesting that F-actin re-organization induced by Hsp90 inhibition was not cell type specific.

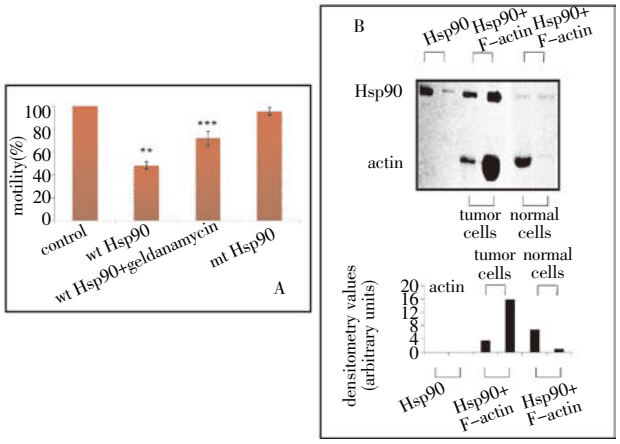

Figure 4. Analysis of Hsp90 binding and interference in acto-myosin motility assay and comparative analysis of Hsp90-actin binding between normal and tumor cells.
A: Analysis of actin motility on myosin coated surface and interference of Hsp90 in the motility. B: Actin binding assay of Hsp90 purified from normal and tumor cells.

3.8. Effect of EGF and cytochalasin D on actin-cytoskeleton

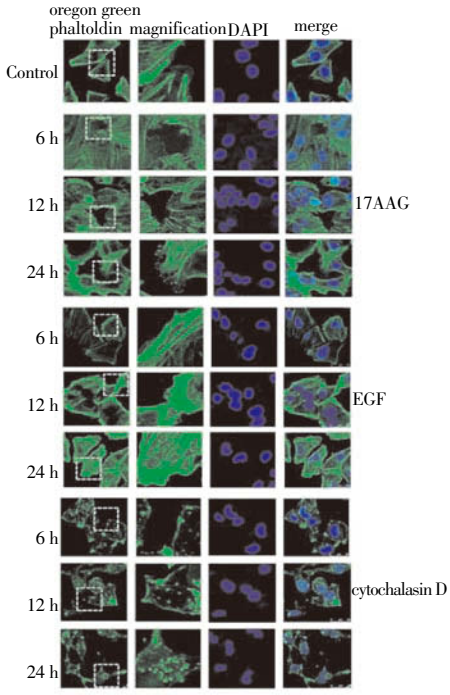

Figure 5. Comparison of 17AAG, EGF, and cytochalasin D induced actin cytoskeleton alterations in human neuroblastoma tumor cells.

Epidermal growth factor (EGF) stimulates actin polymerization whereas actin polymerization inhibitor cytochalasin D inhibits the same. We examined the effect of EGF and cytochalasin D on neuroblastoma either alone or in combination. EGF treatment stimulated actin polymerization exhibiting branched F-actin arrays and its accumulation. Although EGF treatment has induced actin cytoskeleton ruffling, it also enhanced actin bundles on cell periphery. The cytochalasin D treatment has induced actin-depolymerization that resulted in extensive loss of F-actin arrays and actin-bundling. The cytochalasin D combination with EGF resulted in the retention of 50% of actin polymers, and this could be due to the titration effect of EGF on cytochalasin D induced depolymerization after the treatment (Figure 6).

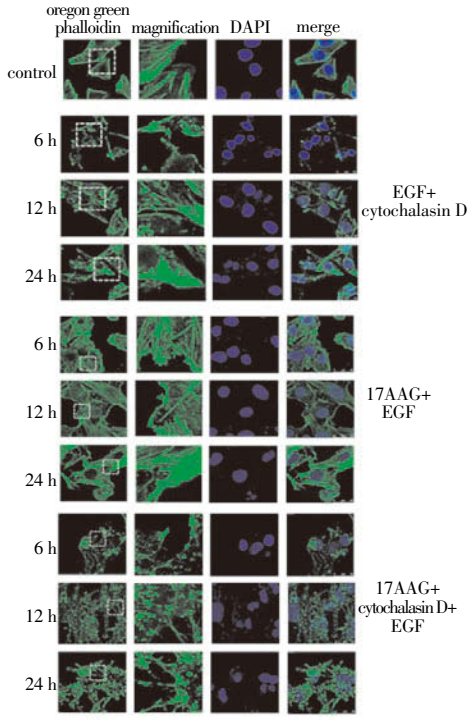

Figure 6. Combinatorial effect induced cytoskeleton alterations in human neuroblastoma cells.

3.9. Effect of 17AAG on EGF and cytochalasin D combination

The 17AAG effect was found to be prominent in destabilizing actin-cytoskeleton, which may relate to the inhibition of actin polymerization or decreased actin content by 17AAG. An extended actin bundles were observed in a time-dependent manner with EGF combination. Similarly cytochalasind D induced loss of actin fibers are retained by EGF combination. When we used cytochalasin D and 17AAG cells lost complete cytoarchitecture due to severe loss and damage to the actin-cytoskeleton (data not shown). A triple combination of 17AAG with EGF and cytochalasin D showed lack of actin cytoskeletal recovery even after prolonged incubation i.e. 24 h. These observations suggested that 17AAG potentiates the effect of cytoskeletal disruptors, and

this effect is not reversible. In our study, 17AAG combination with cytochalasin D resulted in drug induced synergism in both deploymerizing actin and decreasing its content (Figure 6).

4. Discussion

The major finding of the present study is to demonstrate the significance of Hsp90 involvement in the maintenance of tumor cell integrity through stabilizing the actin cytoskeleton. We demonstrate that Hsp90 interacts with F-actin and stabilizes the actin cytoskeleton in tumor cells. We provide information on two important facets, (1) in a cellular system 17AAG induces loss of cellular integrity through actin cytoskeletal destabilization, (2) in a pure system Hsp90 binds to F-actin and only Hsp90 oligomerization appears to enhance actin binding.

Considering the highly organized cytoskeletal proteins and induced expression of Hsp90 in tumor cells, we construe that Hsp90 may be associated with the cytoskeleton. It was shown that Hsp90 inhibition using geldanamycin induces a significant change in membrane polarization and membrane order[23,24]. The cortical F-actin near the plasma membrane is responsible for providing the structural integrity of the cell as well as provide substratum for generating the forces of cellular protrusions, thus actin filament depletion affects transmembrane bending stiffness and equilibrium curvature[25,26]. Although detergent induced cell lysis after 17AAG treatment may not infer 17AAG's direct effect on membrane integrity, provided information that 17AAG treatment sensitizes tumor cells to detergent treatment. The distortion of plasma membrane integrity was further associated with destabilization of actin cytoskeleton. Our findings signify that there was not only a decrease in tension of actin filaments but loss. Thus, 17AAG probably involved in localized relaxation detachment of cortical-cytoskeleton from the plasma membrane.

Our findings demonstrate that Hsp90 binds to both G- and F-actin, however, Hsp90 binding to F-actin especially in tumor cells found to be more alluring. Further, except oligomerization, no other functional modification of Hsp90 showed alterd actin binding. Mapping of actin binding motifs suggested lack of specific actin binding motifs through which Hsp90 can interact with actin[27]. Studies *in vitro*, while allowing defined conditions, suffer from limitations imposed by an artificial environment. However, F-actin interference with luciferase and citrate synthase renaturations added that F-actin binding to Hsp90 may not be through pure hydrophobic interactions as proposed[28]. F-actin assembles with myosin filaments composed of heavy and light chains to form a protein complex that uses energy from ATP hydrolysis to power actin-myosin contraction[29]. Acto-myosin motility assays revealed that Hsp90 binding to actin are not mediated by surface exposed hydrophobic regions and therefore argues against any false interpretation. In addition we now have demonstrated that Hsp90 binding to F-actin is specific to tumor cells, which may be related to the functional status of Hsp90 protein.

The Hsp90 inhibition induced effects on actin-cytoskeleton includes (1) loss of laterally extended F-actin arrays that are in close proximity to the plasma membrane, and (2) distorted bundling of F-actin arrays from straightened actin filaments to twisted/curved form. Prolonged treatment with 17AAG (24 h) showed reappearance of F-actin arrays but that were not in the periphery to plasma membrane but small-spread veins loosely fitted within the cytoplamsic radius. In addition, 17AAG also induced lamellipodia formation on prolonged incubation, however lamellipodia formation may not be significant for cell motility since lamellipodia are rarely observed in cancer cells[30]. The 17AAG induced effects are found to be not cell type specific since these effects were also found in other transformed cells.

EGF stimulates actin nucleation and filament number increase in experimental models[31]. A decrease in F-actin bundling and stress fiber formation in combination with 17AAG suggested that Hsp90 may be indispensible for stress fiber formation and F-actin bundling in tumor cells. Though EGF stimulation was shown to enhance cell proliferation and migration through enhanced actin polymerization[31], we observed a surpassing effect of 17AAG even under conditions of EGF stimulation. Although it was demonstrated that the cellular pool of actin in the polymerized state is not significantly decreased upon cytochalasin D treatment, the disintegration of stress fibers and loss of F-actin arrays and bundles were quite significantly observed in our study. Interestingly, though cytochalasin D treatments were reversible after 24 h (data not presented) its combination with 17AAG resulted in drug induced synergism and found to be irreversible. The triple combination experiments using EGF, cytochalasin D and 17AAG also confirms irrersible effect of 17AAG combination with cytochalasin D.

To enhance the antitumor potential, anticancer drugs are used in combination with certain cytoskeletal disruptors[32,33]. Cytoskeleton disruptors lack selectivity towards tumor cells, hence may affect both normal and tumor cells. Unlike many anticancer drugs, anti-Hsp90 drugs exhibit tumor selectivity[34,35]. Our findings demonstrate that Hsp90 inhibition either alone or in combination with cytoskeletal disruptors induces irreversible damage to the actin-cytoskeleton.

Conflict of interest statement

We declare that we have no conflict of interest.

Acknowledgements

A.S.S expresses thanks to Prof. Peter Csermely and Prof. Soti Csaba for the directive and helpful discussion with the manuscript. Prof. Miklós Kellermayer is accredited for training with acto-myosin experiments. Authors thank Dr. Yoshihiko Miyata for mutated Hsp90, Ms. Nandini Rangaraj for help with confocal microscopy. The work is supported by Department of Biotechnology, Department of Science and Technology, Government of India.

References

[1] Olson EN, Nordheim A. Linking actin dynamics and gene transcription to drive cellular motile functions. *Nat Rev Mol Cell Biol* 2010; **11**: 353-65.

[2] Etienne-Manneville S. From signaling pathways to microtubule dynamics: the key players. *Curr Opin Cell Biol* 2010; **22**: 104-11.

[3] Papakonstanti EA, Stournaras C. Cell responses regulated by early reorganization of actin cytoskeleton. *FEBS Lett* 2008; **582**: 2120-7.

[4] Jiang P, Enomoto A, Takahashi M. Cell biology of the movement of breast cancer cells: intracellular signalling and the actin cytoskeleton. *Cancer Lett* 2009; **284**:122-30.

[5] Chen SM, Meng LH, Ding J.New microtubule-inhibiting anticancer agents. *Expert Opin Investig Drugs* 2010; **19**: 329-43.

[6] Allingham JS, Klenchin VA, Rayment I. Actin-targeting natural products: structures, properties and mechanisms of action. *Cell Mol Life Sci* 2006; **63**: 2119-34.

[7] Kanthou C, Tozer GM. Microtubule depolymerizing vascular disrupting agents: novel therapeutic agents for oncology and other pathologies. *Int J Exp Pathol* 2009; **90**: 284-94.

[8] Kuppens IE.Current state of the art of new tubulin inhibitors in the clinic. *Curr Clin Pharmacol* 2006; **1**: 57-70.

[9] Stirling PC, Cuéllar J, Alfaro GA, El Khadali F, Beh CT, Valpuesta JM, et al. PhLP3 modulates CCT-mediated actin and tubulin folding via ternary complexes with substrates. *J Biol Chem* 2006; **281**: 7012-21.

[10]Brackley KI, Grantham J. Subunits of the chaperonin CCT interact with F-actin and influence cell shape and cytoskeletal assembly. *Exp Cell Res* 2010; **316**: 543-53.

[11]Mashukova A, Oriolo AS, Wald FA, Casanova ML, Kröger C, Magin TM, et al. Rescue of atypical protein kinase C in epithelia by the cytoskeleton and Hsp70 family chaperones. *J Cell Sci* 2009; **122**: 2491-503.

[12]Levitsky DI, Pivovarova AV, Mikhailova VV, Nikolaeva OP.Thermal unfolding and aggregation of actin. *FEBS J* 2008; **275**: 4280-295.

[13]Weis F, Moullintraffort L, Heichette C, Chrétien D, Garnier C. The 90-kDa heat shock protein Hsp90 protects tubulin against thermal denaturation. *J Biol Chem* 2010; **285**: 9525-34.

[14]Jinwal UK, Koren J 3rd, Borysov SI, Schmid AB, Abisambra JF, Blair LJ, et al. The Hsp90 cochaperone, FKBP51, increases Tau stability and polymerizes microtubules. *J Neurosci* 2010; **30**: 591-9.

[15]Wandinger SK, Richter K, Buchner J. The Hsp90 chaperone machinery. *J Biol Chem* 2008; **283:** 18473-7.

[16]Hahn JS. The Hsp90 chaperone machinery: from structure to drug development. *BMB Rep* 2009; **42**: 623-30.

[17]Hwang M, Moretti L, Lu B. HSP90 inhibitors: multi-targeted antitumor effects and novel combinatorial therapeutic approaches in cancer therapy. *Curr Med Chem* 2009;**16**: 3081-92.

[18]Mahalingam D, Swords R, Carew JS, Nawrocki ST, Bhalla K, Giles FJ. Targeting HSP90 for cancer therapy. *Br J Cancer* 2009; **100**: 1523-9.

[19]Butcher DT, Alliston T, Weaver VM. A tense situation: forcing tumour progression. *Nat Rev Cancer* 2009; **9**:108-22.

[20]Gieni RS, Hendzel MJ. Actin dynamics and functions in the interphase nucleus: moving toward an understanding of nuclear polymeric actin. *Biochem Cell Biol* 2009; **87**: 283-306.

[21]Luikart SD, Panoskaltsis-Mortari A, Hinkel T, Perri RT, Gupta K, Oegema TR, et al. Mactinin, a fragment of cytoskeletal alpha-actinin, is a novel inducer of heat shock protein (Hsp)-90 mediated monocyte activation. *BMC Cell Biol* 2009; **10**: 60.

[22]Tucker NR, Shelden EA. Hsp27 associates with the titin filament system in heat-shocked zebrafish cardiomyocytes. *Exp Cell Res* 2009; **315:** 3176-86.

[23]Didelot C, Lanneau D, Brunet M, Joly AL, De Thonel A, Chiosis G, et al. Anti-cancer therapeutic approaches based on intracellular and extracellular heat shock proteins. *Curr Med Chem* 2007; **14**: 2839-47.

[24]Sehgal PB. Plasma membrane rafts and chaperones in cytokine/STAT signaling. *Acta Biochim Pol* 2003; **50**: 583-94.

[25]Römer W, Pontani LL, Sorre B, Rentero C, Berland L, Chambon V, et al. Actin dynamics drive membrane reorganization and scission in clathrin-independent endocytosis. *Cell* 2010; **140**: 540-53.

[26]Saarikangas J, Zhao H, Lappalainen P. Regulation of the actin cytoskeleton-plasma membrane interplay by phosphoinositides. *Physiol Rev* 2010; **90**: 259-89.

[27]Su Y, Kondrikov D, Block ER. Beta-actin: a regulator of NOS-3. *Sci STKE* 2007; **2007**: pe52.

[28]Pratt WB, Morishima Y, Peng HM, Osawa Y. Proposal for a role of the Hsp90/Hsp70-based chaperone machinery in making triage decisions when proteins undergo oxidative and toxic damage. *Exp Biol Med* (Maywood) 2010; **235**: 278-89.

[29]Naumanen P, Lappalainen P, Hotulainen P. Mechanisms of actin stress fibre assembly. *J Microsc* 2008; 231: 446-54.

[30]Machesky LM. Lamellipodia and filopodia in metastasis and invasion. *FEBS Lett* 2008; **582**: 2102-11.

[31]Kimura F, Iwaya K, Kawaguchi T, Kaise H, Yamada K, Mukai K, et al. Epidermal growth factor-dependent enhancement of invasiveness of squamous cell carcinoma of the breast. *Cancer Sci* 2010;**101**: 1133-40.

[32]Lassen U, Molife LR, Sorensen M, Engelholm SA, Vidal L, Sinha R, et al. A phase I study of the safety and pharmacokinetics of the histone deacetylase inhibitor belinostat administered in combination with carboplatin and/or paclitaxel in patients with solid tumours. *Br J Cancer* 2010; **103**:12-7.

[33]Engert A, Franklin J, Eich HT, Brillant C, Sehlen S, Cartoni C, et al. Two cycles of doxorubicin, bleomycin, vinblastine, and dacarbazine plus extended-field radiotherapy is superior to radiotherapy alone in early favorable Hodgkin's lymphoma: final results of the GHSG HD7 trial. *J Clin Oncol* 2007; **25**: 3495-502.

[34]Kabakov AE, Kudryavtsev VA, Gabai VL. Hsp90 inhibitors as promising agents for radiotherapy. *J Mol Med* 2010; **88**: 241-7.

[35]Hwang M, Moretti L, Lu B. HSP90 inhibitors: multi-targeted antitumor effects and novel combinatorial therapeutic approaches in cancer therapy. *Curr Med Chem* 2009; **16**: 3081-92.